PCCP

Accepted Manuscript

ROYAL SOCIETY OF CHEMISTRY

www.rsc.org/pccp

Observation and Manipulation of Hexa-Adamantyl-Hexa-Benzocoronene Molecules by Low Temperature Scanning Tunneling Microscopy†

Bastien Calmettes,[a] Loranne Vernisse,[a] Olivier Guillermet,[a] Youness Benjalal,[a] Xavier Bouju,[a] Christophe Coudret,[b] and Roland Coratger*[a]

Received Xth XXXXXXXXXX 2014, Accepted Xth XXXXXXXXX 2014
First published on the web Xth XXXXXXXXXX 2014
DOI: 10.1039/b000000x

Large molecules made of a central hexabenzocoronene plateau surrounded by six adamantyl groups have been investigated by low temperature scanning tunneling microscopy and scanning tunneling spectroscopy coupled with image calculations and molecular mechanics. The structure of large self-assembled domains reveals that the intermolecular interactions between adamantyl peripheral groups dominate film growth. At very low coverage, the molecules can present a certain instability for negative bias voltages which induces a partial rotation. Manipulations of single objects using the STM tip are used to create small clusters of two or three molecules. The formed structures can be obtained and manipulated provided that the flexible adamantyl moieties of neighbouring molecules are brought in close contact promoting a robust mechanical anchoring.

1 Introduction

The large molecules are good candidates for the elaboration of nanostructures with predictable physical and chemical characteristics[1]. However, these characteristics and the potential applications that may result, assume that their behaviour on a substrate is well known which is far from being simple. Among these molecules, coronene and particularly hexa-peri-hexabenzocoronene (HBC) have been intensively studied. They belong to the class of polycyclic aromatic hydrocarbons which can be regarded as small graphite parts, sometimes called nanographene[2,3]. As these molecules are planar, their adsorption geometry is generally predictable except when the substrate is a vicinal surface[4]. In this case, the molecules are tilted after adsorption at the step edge. Otherwise, their ability to form self assembled domains has been largely demonstrated on HOPG graphite[5], Si(111)7×7[6], Cu(111)[7], Au(100)[8], Ag(111)[9]. Another interesting property of these compounds is their ability to be linked to peripheral groups able to exhibit a peculiar property. For example, Jäckel *et al.*[10] and Watson *et al.*[11] present rectifying behaviours of functionnalized HBC molecules at the solid-liquid interface.

In this paper, hexa-adamantyl-hexabenzocoronene molecules (Ad_6HBC, see Fig. 1) have been observed using low temperature scanning tunneling microscopy (LT-STM) after adsorption on Ag(111). These molecules, specifically synthesized, present the particularity to include carbon atoms in two hybridization state: a central sp^2 plateau and six peripheral groups in which carbon atoms are sp^3 hybridized. The investigations have been performed on self-assembled domains as well as on single molecules. STM image calculations suggest that the molecular states are substantially decoupled from the substrate thanks to the peripheral adamantyl groups and that the contrast variations inside the Ad_6HBC can be correctly interpreted. For isolated objects, lateral manipulations with the STM tip demonstrate that it is possible to build small stable dimers or trimers.

2 Experimental details and computational methods

The experiments have been conducted on a scanning tunneling microscope (STM) working at liquid helium temperature ($T = 4.5$ K) (LT Omicron) and with a base pressure of 2×10^{-11} mbar. The Ag(111) crystal is cleaned by repeated Ar^+ bombardment cycles at $E = 600$ eV followed by annealing at 800 K for 1 hour. The Ad_6HBC molecules are deposited on a W filament 0.15 mm in diameter and then, are pumped by a turbo molecular pump

[a] *CEMES / UPR 8011 CNRS and Université Paul Sabatier, Nanoscience Group, 29 rue J. Marvig BP 94347, 31055 Toulouse France. E-mail: coratger@cemes.fr*
[b] *IMRCP, Université Paul Sabatier, 118 route de Narbonne, 31062 Toulouse France.*

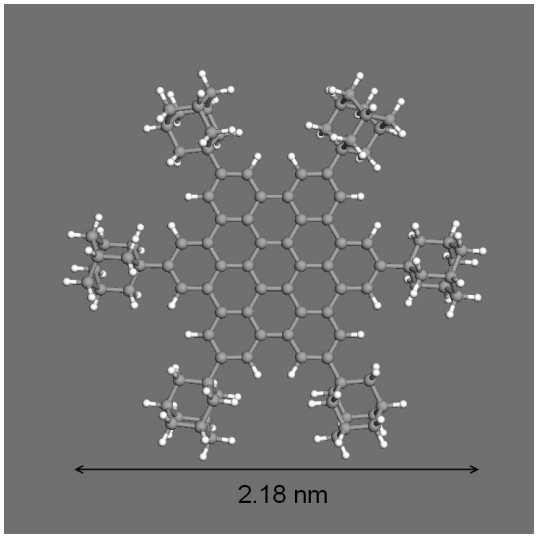

Fig. 1 Chemical structure of an hexa adamantyl hexa benzocoronene (Ad_6HBC) molecule (H atoms are in blank and C atoms in grey).

during more than 12 hours. The filament is submitted to high temperature outgassing cycles before evaporation. In a first set of experiments, the substrate was held at room temperature in the preparation chamber. These experiments have been used to probe the self-assembly properties of the molecules which are evaporated at rates of about half a monolayer per minute. In the second set of manipulations, the molecules are directly evaporated on the STM head through a small hole 1 mm in diameter drilled in the He cryostat. The Ag(111) sample is then held at 4.5 K during the evaporation so that thermal diffusion is inhibited. In addition, small evaporation rates in the 1/1000 monolayer range per minute can be easily achieved. These conditions are used for single molecule experiments. Tips made of tungsten wires 0.2 mm in diameter were prepared by electrochemical etching and cleaned in UHV using direct current heating. The bias voltage is applied to the sample.

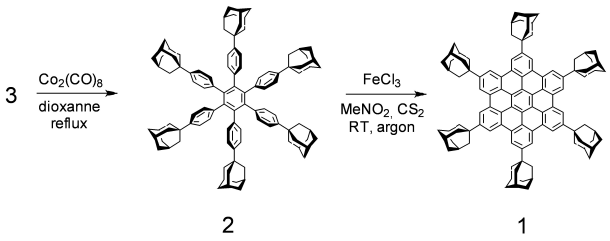

Fig. 2 Synthesis of compound 2 hexa-(p-adamantylphenyl benzene) and 1 *peri*-hexa adamantylbenzocoronene (Ad_6HBC).

Synthesis of compounds 1 and 2 is outlined in Fig. 2, and involved classical approach of such polyaromatics[12]. *Peri*-hexa-adamantylhexabenzocoronene was prepared by the Scholl oxidative cyclodehydrogenation of the hexaphenylbenzene precursor 2. Due to its poor solubility a mixture of solvent including carbon disulfide was employed. The high symmetry of compound 2 prompted us to use the cobalt-catalyzed cyclotrimerization of the tolane 1,2 -di-[4'-(1"-adamantyl)-phenyl]acetylene 3. Eventually, this symmetrical tolane 3 was prepared by a double Sonogashira reaction involving acetylene gas (Fig. 3)[13,14] but using $Pd(PPh_3)_4$, a palladium (0) precatalyst, and hydroquinone in order to limit the apparition of Glaser-type products. 1-(para-iodophenyl) adamantane and its precursor 1-phenyladamantane were obtained without difficulties following or adapting literature procedures[15,16]. Details of the characterisation data of compounds 1 and 2 are given in the Supplementary Information file.

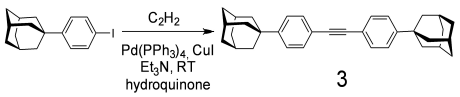

Fig. 3 Synthesis of the tolane precursor 3.

Calculations of the molecular conformation on the Ag(111) surface were performed by using the force field provided by the MM4 code[17,18]. This molecular mechanics technique has already demonstrated its efficiency to describe the adsorption of polyaromatic hydrocarbon or organo-metallic molecules on metallic surfaces[19–21]. Indeed, the molecules are physisorbed and no reactive effects have to be described for chemical bonding. This justifies the use of such a method. Moreover, each molecule is constituted of 204 atoms and we have considered a slab of two or four layers to described the substrate. The total number of atoms precludes the use of DFT-like methods due to a prohibitive computational cost. The calculated STM images were obtained using the elastic scattering quantum chemistry (ESQC) code[22], which is a powerful and accurate technique. Starting with the MM4 optimized conformations, the ESQC-STM images can be compared with experimental ones with good agreement[23–25].

3 Results

3.1 Structure of the self-assembled network

First, Ad_6HBC molecules have been deposited on the Ag(111) surface held at ambient temperature and formed

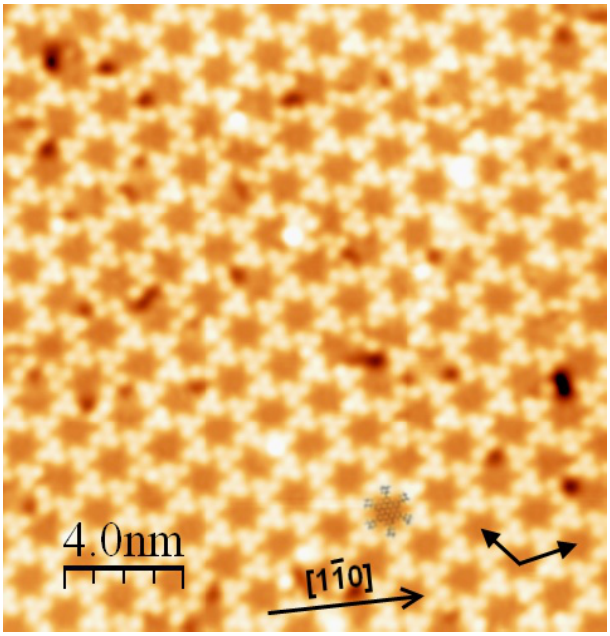

Fig. 4 STM image 20 × 20 nm^2 of the Ad$_6$HBC self-assembly after room temperature evaporation. The molecular structure of Ad$_6$HBC as well as the [110] type direction of the substrate have been superimposed. V_s=1.5 V, I_t=100 pA, T=4.5 K

a self-assembled network. A large scale image 20 × 20 nm^2 is presented in Fig. 4. Each molecule exhibits six characteristic bumps and a central plateau with a lower corrugation. The molecular network presents an hexagonal Bravais lattice with a parameter of 1.77 nm. The apparent height of the molecule layer with respect to the underlying metallic substrate is about 0.17 nm at this bias voltage. This apparent height is different from the real height of the molecule which could be expected from its chemical structure. It corresponds to the corrugation as measured by the STM tip and is related to the tunneling current and to the electronic properties of the object.

A close inspection also reveals that the network is disoriented with respect to the [110] type directions of the Ag surface. This suggests a low interaction with the metal and an absence of commensurability between the molecular monolayer and the surface lattice. Some defects can be also observed. They appear as black holes with a 0.1 nm depth with respect to the top layer for the deepest. These defects correspond to the absence of one, two or more rarely three bumps around the central plateau. It can therefore be assumed that the six maxima surrounding the central part of the molecules correspond to the six adamantyl (AD) groups and that some molecules lose one of these groups during the evaporation process. The mass spectra presented in the supplementary materials confirm the purity of the final compound and also confirm that the fragmentation of some molecules only occurs during the deposition. However, these defects are of small importance in the network formation. Two or three of AD groups are sufficient to guide each molecule in the structure as can be observed in Fig. 4, even if one or two adamantyl are missing. Then, all the molecules have the same orientation in the self-assembly. This point will be also discussed in the part devoted to single molecule experiments.

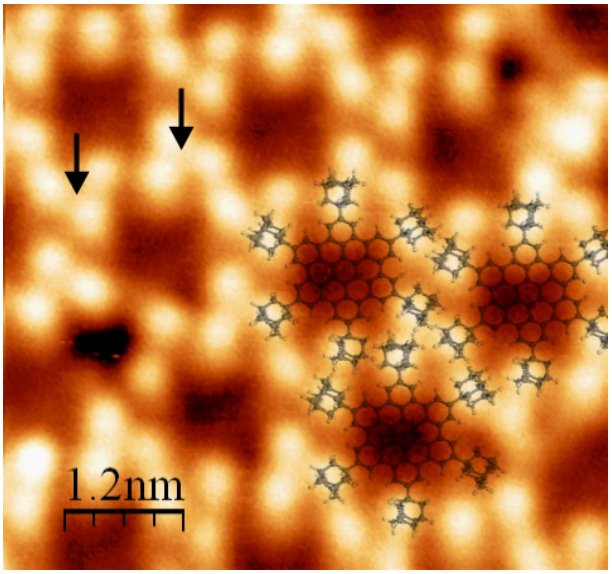

Fig. 5 STM images (6 × 6 nm^2) of the Ad$_6$HBC network and proposed model for the self-assembly. V_s=1.5 V, I_t=10 pA, T=4.5 K

A close-up view of the molecular layer is presented in Fig. 5 where the molecular geometry has been superimposed. It appears that the structure implies a certain degree of interlocking between adamantyl groups. These latter seem to form trimers between neighbouring molecules indicated by black arrows in Fig. 5. This explains that the lattice parameter of the self-assembly is slightly smaller as compared to the total size of the Ad$_6$HBC (typically, 2 nm from one carbon to an opposite one in gas phase). The smallest distance between two adjacent adamantyl groups is 0.46 nm in the lattice while this carbon cage is about 0.3 nm in diameter. The low corrugation observed within the molecular layer (0.05 nm) is related to the small height of the adamantyl top with respect to the central HBC plateau.

3.2 Observation of single molecules

Using evaporation at very low rates on an Ag substrate held at low temperature, it is possible to observe single Ad_6HBC molecules.

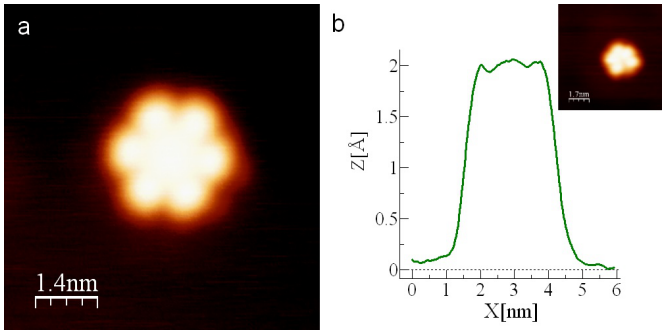

Fig. 6 a) STM images (7×7 nm^2) of a single Ad_6HBC molecule and b) cross section along the molecule. The insert shows a Ad_5HBC structure V_s=1.5 V, I_t=13 pA, T=4.5 K

As expected from the molecular model, a single molecule presents a characteristic sixfold geometry (Fig. 6a). Its apparent height on the Ag(111) surface is about 0.2 nm (Fig. 6b). This value has to be compared to the mean diameter of each adamantyl group which is estimated to be about 0.5 nm from the chemical structure. As previously explained, this difference is due to a well-known electronic effect related to the molecular electron states and the low values of the tunneling current used in these experiments. The total diameter of the molecule is 2.6 nm which is more important than in the self-assembly (1.85 nm). In this case, the STM tip overestimates the object size. At 1.5 V, the central part of the molecule shows a slightly higher corrugation than the surrounding AD groups (Fig. 6b), which means that the central plateau provides the largest contribution to the tunneling current. For high positive values (typically above 2 V) and for small negative voltages (typically above -1 V), the six AD moieties present the largest corrugation as in Fig. 5. During the experiments performed on single molecules, some molecular objects with five maxima (sometimes less) have been observed (see insert in Fig. 6). Therefore, the instability of a few molecules during the evaporation process is again observed at the single molecule level. This result is also confirmed by the presence of small circular particles about 0.16 nm in height and 1.1 nm in diameter on the surface. These latter correspond to the adamantyl moieties which have been separated from the molecular entities.

More surprisingly, when a negative voltage below -1 V is used, the molecules can present an unexpected shape. An example is presented in Fig. 7. It appears that instead of a sixfold geometry, the molecule exhibits twelve maxima while the apparent height as well as the mean diameter remain the same. Thus, the STM images appear slightly noisy but the result is very reproducible and the general shape never changes. The transition to a positive bias voltage stabilizes the molecule and this latter recovers its hexagonal structure.

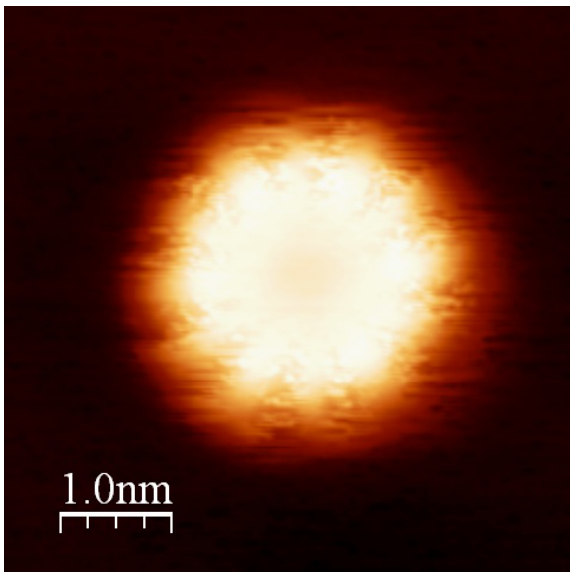

Fig. 7 STM image (5×5 nm^2) of a single Ad_6HBC observed at negative bias voltage. V_s=-1.5 V, I_t=75 pA, T=4.5 K

To complete the characterization, tunneling spectroscopy experiments have been conducted on single molecules. For this, $I(V)$ spectra have been performed on the Ag(111) surface and on the two main important parts of the molecule, i.e. the central plateau and the peripheral adamantyl groups. The derivatives dI/dV of the $I(V)$ curves have been numerically calculated and are presented in Fig.8.

Several points can be highlighted. Firstly, the curve obtained on the Ag(111) surface exhibits the characteristic threshold at about 0.07 eV below the Fermi level due to the well known electronic surface state[26]. This feature reveals the metallic character of the tip. The presence of two peaks at -1.44 eV and -1 eV is attributed to tip electronic states. This contribution has been numerically subtracted from the curves recorded on the molecules. When the dI/dV are recorded on the adamantyl group, the spectrum shape is different. Below the Fermi level, a new structure at -1.28 eV is now observed and a second peak appears at -1.65 eV. Above the Fermi level, the modification is more important. The spectrum exhibits a broad structure with a first maximum around 0.34 eV and a second around 0.83 eV. The last structures are

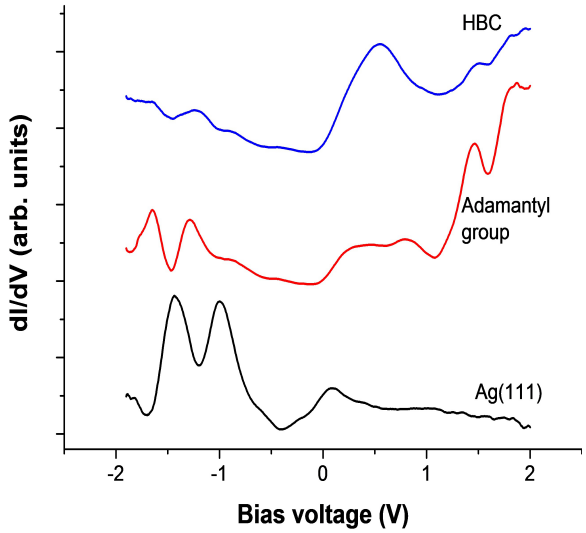

Fig. 8 STS experiments performed on the Ag(111) surface (black curve), the adamantyl groups (red curve) and the central plateau (blue curve) V_s=-1 V, I_t=5 pA, T=4.5 K.

centred at about 1.46 eV and 1.82 eV respectively. As compared to the data recorded on the Ag surface, it can be concluded that the AD groups mainly contribute to the empty states. When the experiments are conducted on the central HBC plateau, the two structures at -1.28 eV and -1.65 eV are broadened. Above the Fermi level, the two peaks at 0.34 eV and 0.83 eV are replaced by a shoulder at about 0.2 eV and a very large peak centred at 0.54 eV. The intensity of the peaks at 1.46 eV and 1.82 eV slightly decreases but the two structures are still observed. Then, it can be concluded that the contribution of the central plateau to the empty states is most important just above the Fermi level as compared to the spectrum obtained on the adamantyl moieties.

3.3 Manipulation of single molecules

The presence of adamantyl groups around the HBC structure makes the molecule easier to be manipulated on a metallic substrate. Indeed, these peripheral groups decrease the strength of the π interactions of the central coronene with the metal. To check this hypothesis, single molecules have been manipulated using the STM tip. For this, the tip is approached towards the surface of 3.2 Å and the feedback loop is disengaged. The tip is then moved at constant height relative to the substrate along a predefined path and the induced variations of the tunneling current are recorded as a function of time[27]. By recording the tunnel current during the manipulation, that is to say with respect to a lateral coordinate of the tip, one gets curves showing specific signatures according to the manipulation mode[28–30]. An example of such a manipulation is reported in Fig. 9.

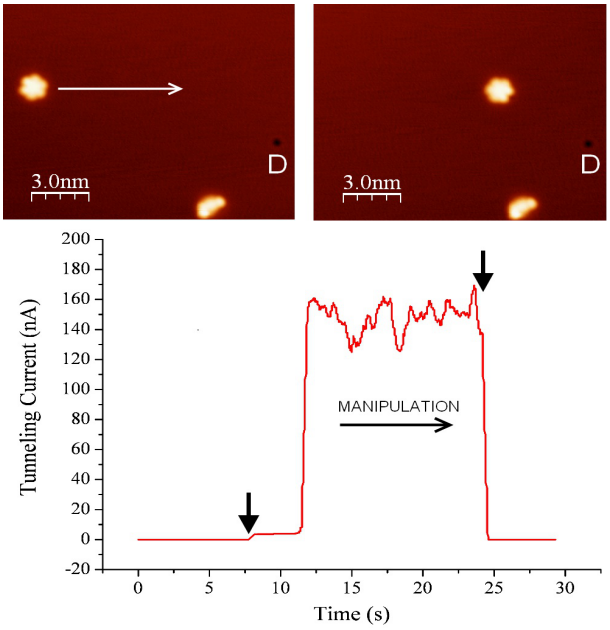

Fig. 9 Lateral manipulation of an Ad_6HBC molecule using the STM tip and variations of the tunneling current during the experiment (the sequence of manipulation is indicated by the two vertical arrows) V_s=1 V, I_t=5 pA, T=4.5 K.

The two STM images show a Ad_6HBC before (left) and after (right) the manipulation process. A small defect on the Ag(111) surface and called D as well as a fragment of another molecule are used as reference. The curve presents the variations of the tunneling current during the molecule displacement and the two arrows indicate the moment where the tip is approached from 3.2 Å towards the surface for manipulation. In a first step, the tunneling current increases from 5 pA to 3.7 nA due to the smaller tip-sample distance. As the tip approaches the molecule, the current rises up to 150 nA and the molecule is displaced using the pushing mode. As compared to the signal recorded during manipulations of small molecules[31–33], the data produced by Ad_6HBC are more complex. This is characteristic of the displacement of a large molecule containing more than 200 atoms which probes a large amount of substrate atoms during its motion and has a large number of degrees of freedom[34]. The behaviour of Ad_6HBC is even more complicated to analyse if one considers the possibility of molecular deformation and rotation of adamantyl groups. Indeed, a careful observation of the molecule before and after the

manipulation shows that it has rotated of at least 30°. Even when the molecule is displaced along [110] type direction of the substrate, it is difficult to record a periodic signal, contrary to Lander molecules for example. Indeed, manipulation signatures have complex features as the number of degrees of freedom is increased. However, the experiments performed in the pushing mode are highly reproducible and the displacements are performed with a great accuracy whatever the chosen direction.

Afterwards, the experiments have been performed using several molecules. Indeed, the reproducibility of the manipulation experiments allow the creation of dimers or trimers which in turn can be manipulated. In a first series of experiments, two single molecules have been simply approached each other so that their adamantyl groups are in contact. The intermolecular distance is then 0.5 nm from center to center which is close to the distance observed in the self-assembly where van der Waals interactions dominate. Then, this dimer is manipulated using the pushing mode. Most of the time, the dimer is unstable and the molecules separate while attempting to manipulate them together. This is not surprising since there is no chemical bond between them. The formed structure is stable when the first manipulation is performed until the two Ad_6HBC are in close contact, creating an interlocking between them. In this case, the dimer presents the structure shown in Fig. 10.

The apparent height of the structure is 0.28 nm. The distance between the molecule centres is about 0.94 nm which means that the two objects are now closer than in the self-assembly presented in Fig.5. Then, the mechanical interaction with the tip during the manipulation process induces the creation of a stable dimer in which each molecule is sufficiently deformed to engage a solid connexion due to the flexibility of its peripheral AD groups. The small deformation of the two molecules after contact can be detected in the current variations (Fig. 10c) as a sudden increase of about 50 nA. This mechanical interaction is extremely strong and it is possible to manipulate the dimer on the surface without breaking it: the assembly is perfectly rigid and no fragmentation is observed. On the other hand, the stability of the structure increases. As a consequence, the motion presented in Fig. 7 for a single molecule is prohibited and cannot be observed for the dimers whatever the used bias voltage.

The last manipulation concerns the formation of a trimer using the same method. After the formation of a dimer presenting the suitable structure, a third molecule is manipulated towards the dimer using the method already described. The formed trimer is stable provided that it presents the structure presented in Fig. 11. Thereafter, it can be manipulated on the surface using the pushing mode.

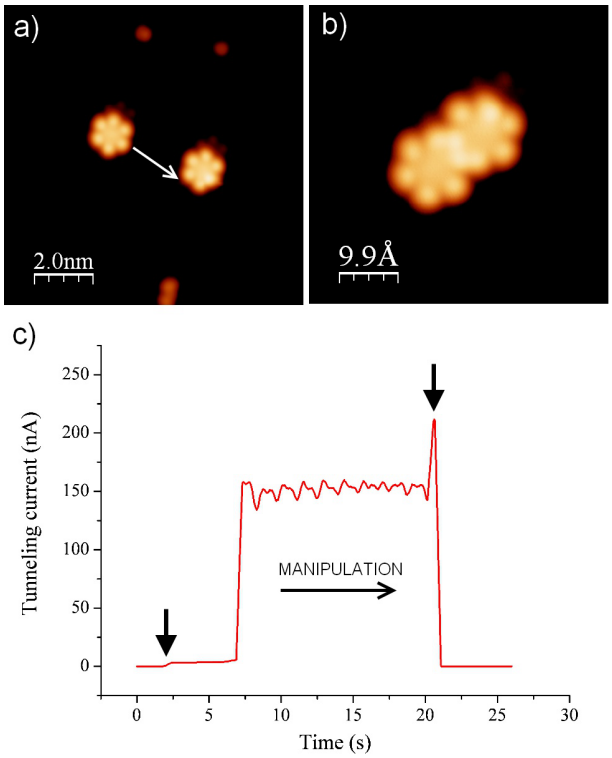

Fig. 10 a) STM image of two Ad_6HBC molecules and b) formation of a dimer using lateral manipulation with the STM tip. c) Variations of the tunneling current during the experiment V_s=1.6 V, I_t=10 pA, T=4.5 K.

Its apparent height is very similar to the one of the dimer (0.29 nm) but the molecules do not form a real equilateral triangle. The smaller distance is 0.94 nm but the two other intermolecular distances are 0.96 nm and 1.01 nm respectively. Indeed, the assembly is driven by mechanical interactions which discard the formation of geometric structures generally induced by chemical bonding.

It is possible to disassemble the cluster using a reduced tunneling resistance of 3.5 MΩ and scanning the triangular structure along one of its heights. When the tip reaches the central maximum, the molecule whose center will be scanned, is removed from the trimer (see Fig. 12). It can be observed that none of these manipulations leads to fragmentation of Ad_6HBC.

4 Discussion

After evaporation on a substrate held at room temperature, the Ad_6HBC molecules self-assemble to form a well defined hexagonal lattice related to the sixfold symme-

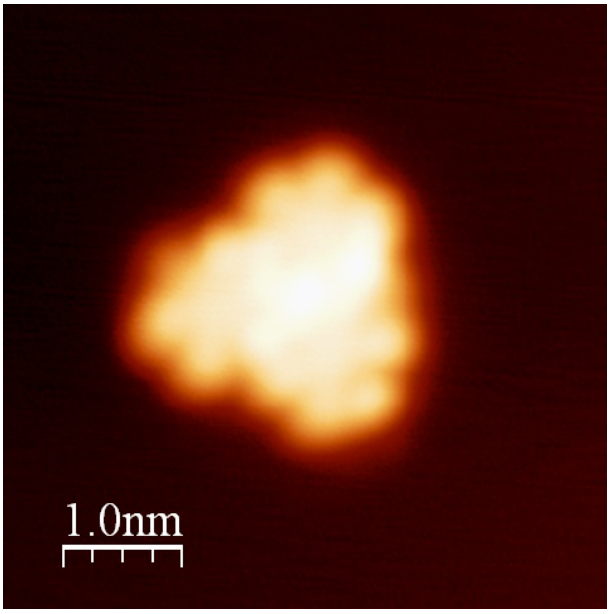

Fig. 11 STM image of three Ad_6HBC forming a trimer after lateral manipulation V_s=1.2 V, I_t=5 pA, T=4.5 K.

try of the molecule. Coronene and related molecules also present hexagonal lattices on different substrates such as HOPG graphite[5], Au(100)[8], Cu(111)[7] and Ag(111)[9] and even in liquids[11]. On Ag(111), coronene molecules are slightly tilted with respect to the substrate which minimizes the π interactions with the metallic atoms and increases the intermolecular ones inside the layer[9]. Van der Waals interactions generally drive these self-assemblies[7]. For Ad_6HBC, the same interactions are responsible of the observed structures. The interactions inside the layer are substantially increased due to the presence of the six adamantyl groups surrounding each HBC centres. It has been already observed that these 3D moieties favours the intermolecular interactions in the self-assembled layers of adamantyl hexa-phenyl benzene molecules (Ad_6HPB) deposited on Ag(111)[35]. This property also explains that the orientation of the Ad_6HBC layer is not related to the close packed directions of the substrate while the molecule size prevents any commensurability with the Ag lattice.

However, the molecules slightly interact with the surface leading to a slight deformation of its structure. To determine the precise adsorption geometry, molecular mechanics calculations have been performed using MM4 software. The results are shown in Fig. 13. It can be observed that the link between the central core and each AD group is flexible and that the carbon-hydrogen bondings pointing toward the surface prevent a strong interaction

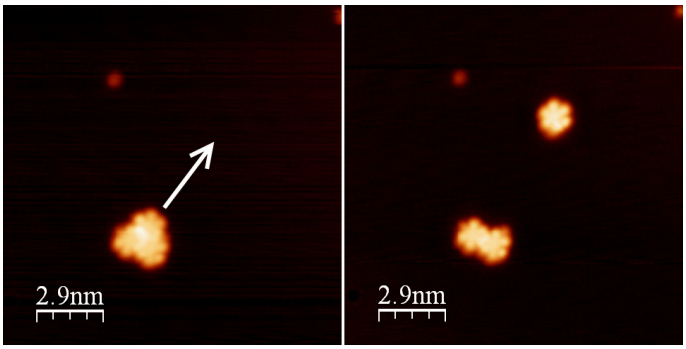

Fig. 12 STM image of three Ad_6HBC after separation of the trimer using lateral manipulation. The arrow indicates the scan direction used for manipulation V_s=1.2 V, I_t=5 pA, T=4.5 K.

between the HBC and the substrate.

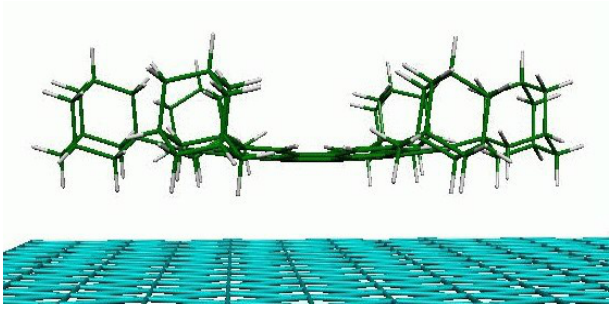

Fig. 13 Calculated adsorption geometry of Ad_6HBC on the Ag(111) substrate. Ag atoms are presented in blue.

Furthermore, due to the presence of the AD peripheral groups which act as spacer legs, the π interactions between the central plateau and the Ag surface induce a small bending of the HBC part. The mean molecule-substrate distance is 3.8 Å. For the central benzene ring, the C-Ag distance is 2.68 Å while this value reaches 3.45 Å for the most peripheral carbon atoms of the HBC part. The smallest calculated H-Ag distance is around 2.0 Å for the hydrogen atoms of the adamantyl groups. One may guess that this small lift-up due to the presence of the interlaying hydrogen atoms will have an impact to the diffusion barrier compared to the a bare HBC molecule. Simultaneously, the peripheral AD groups bend upwards because of the hydrogen atoms interacting with the metal. As compared to hexa-adamantyl-hexa-phenyl benzene molecules previously studied[35]), a more important decoupling is expected to take place because of the rigidity of the central HBC part as compared to HPB. This decoupling explains the ability to move the molecule as compared to the high stability of the

Ad_6HPB in the same tunneling conditions. On the other hand, the π coupling is also more important because of the flat structure of the nanographene part. Then the adsorption geometry results from a subtle balance between these two opposites effects. The molecules interact with the metallic substrate inducing a slight bending but this interaction is reduced due to the adamantyl legs. Furthermore, the AD groups favour the intermolecular interactions within the layer and the building of very robust self-assemblies[36]. The molecule-substrate interaction is less important and does not play any role in the domain formation. As compared to the supramolecular phase observed with adamantyl hexa-phenyl benzene molecules ([35]), Ad_6HBC layers exhibit a mechanical interaction between the peripheral group which has not been previously observed. Indeed, while the Ad_6HPB networks are formed with neighbouring molecules simply in contact (the lattice periodicity is about 2.1 nm), Ad_6HBC domains are build after the intermixing of adamatyl groups which results in smaller intermolecular distances (1.77 nm).

STM images of single molecules reveal the six adamantyl groups which exhibit the most important corrugation, especially at negative bias voltages. This result is expected since these groups dominate the central plateau after its deformation induced by adsorption (Fig. 13). Using the optimized geometry obtained by MM4, STM image calculations have been conducted using the ESQC software and are reported in Fig. 14.

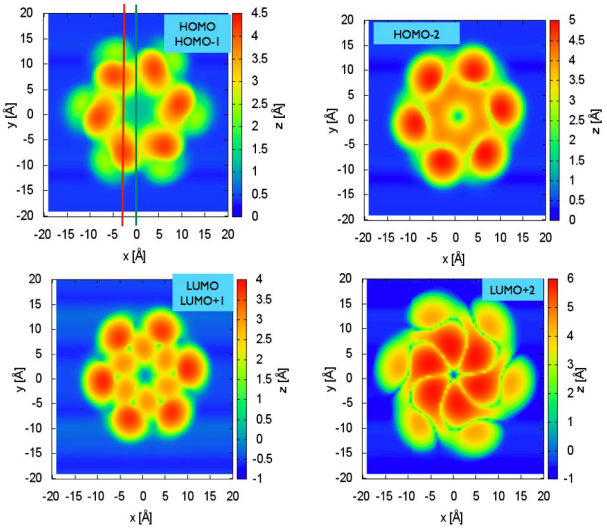

Fig. 14 Calculated ESQC-STM images of the Ad_6HBC molecule on Ag(111) surface at different energies from letf to right and top to bottom, −0.11 eV, −0.53 eV, +1.74 eV and +1.89 eV.

With an energy of −0.11 eV below E_F, corresponding to the HOMO and HOMO−1 states that are degenerated, the calculated image shows a six-fold symmetry with lateral traces of the AD groups. The total calculated corrugation is about 3.6 Å, and the internal corrugation between the HBC core and one AD group is about 3 Å. Details of the corrugation measurement are given in the Supplementary Information file. At an energy of −0.53 eV (HOMO−2), the calculated image has always six pronounced bumps. Then, for positive energies, the images at +1.74 eV and +1.89 eV correspond to the LUMO/LUMO+1 and LUMO+2, respectively. Here, one always observes a six-fold symmetry with a much more important contribution at the center of the molecule.

For a positive polarisation above +1 V, the HBC and AD parts almost presents the same corrugation. This corrugation significantly increases above 2 V and then, the molecules exhibit a single maximum, the main contribution to the tunneling current originating from the coronene moiety. As mentioned, ESQC results suggest the same evolution (Fig. 14). Indeed, the calculations performed using the LUMO+1 and LUMO+2 states show a corrugation increase in the central part meaning that these electronic states significantly contribute to the tunneling current. Since the ESQC images are calculated at a given energy (for example 1.89 eV above E_F for the image in the lower right corner of Fig. 14), they can be slightly different from the experimental images which have been obtained after integrating the tunneling electrons over an energy window in the E_F to $E_F + eV$ range. Thus, the experimental images can be seen as the continuous sum of the calculated ones in this energy range. The simple sum of the two LUMO's images (LUMO/LUMO+1 and LUMO+2) clearly shows that the contribution from the central HBC part increases and may dominate when these states are involved in the tunneling current. This is in good agreement with the experimental results obtained at high positive voltage. In previous investigations, the same conclusions have been drawn from the observation of Ad_6HPB molecules deposited on Ag(111)[35]. In this case, the six adamantyl moieties also presented the highest corrugation. The central benzene then showed a small minimum except at high voltage (typically above 3V) where the whole molecule exhibited a single maximum centred on the HPB part.

The spectroscopic investigations reported in Fig. 8 also reveal the electronic properties of these molecules and explain the contrast variations in terms of applied voltage. On the adamantyl groups as well as on the HBC plateau, the onset of the metallic surface state at 70 meV below E_F disappears. Then, the two different parts of the molecule (HBC and AD) retain specific electronic proper-

ties as compared to the substrate. Below the Fermi level, the contributions at −1.28 eV and −1.65 eV mainly appear on the AD moieties. Above, the large structure at +0.54 eV detected on the HBC part is less marked on the AD moiety. Finally, the two peaks at 1.44 and 1.78 eV are observed on AD and appear as small shoulders on the central carbon part. It can be concluded that these features are due to the molecular electronic structure. Particularly, it is assumed that the peak at -1.28 eV below (contribution from the AD moiety) and the large structure above the Fermi level (contribution from the HBC part extending over about 1 eV) are related to the HOMO-LUMO states of Ad_6HBC. This observation is also consistent with the calculated and experimental STM images showing the large contribution of the AD parts below the Fermi level and the increasing role of the HBC structure above E_F. A gap of 1.82 eV is then estimated from spectra of the Ad_6HBC molecules adsorbed on Ag(111). The EHMO approach within the ESQC code also allows the calculation of the HOMO-LUMO gap and a value of 1.85 eV has been determined, in good agreement with the experimental data.

Some STM images also show that twelve-fold structures can be observed (Fig. 7). Due to the six-fold structure of the molecule, such a geometry can be explained by a small rotation below the tip apex. To answer this question, MM4 investigations have been performed in order to calculate the rotation barrier height when the molecule lies on different adsorption sites (top, bridge and hollow). This is considered in Fig. 15. The curves describe the adsorption energy variation for the three sites by considering a relaxed molecule with all the degrees of freedom free to relax except a single reference atom for which the (x, y) coordinates are kept frozen for each rotation. The most favourable position is above the hollow site (point A) and switches to the atop site when the molecules rotates of 30 degrees (point C) crossing the potential energy point B. The distance between the two sites is small (1.7 Å) as compared to the size of the molecule. Thus, the observed instability is related to the small lateral motion of the molecule while the tip induced rotation shows up the twelve-fold structure. This motion/rotation seems strongly linked to the electric field applied by the STM tip since a negative bias voltage is necessary to engage this phenomenon. In Fig. 15, the curves have to be considered as particular traces extracted from the full potential energy surface. This former should exhibit complicated features due to the numerous degrees of freedom of the system. Moreover, the presented MM4 calculation does not include the presence of the tip nor the local electrostatic field. These two terms probably break the apparent symmetry of the energy barriers of rotation, so that the molecule stays in the neighbourhood of the main hollow site, preventing a net displacement to adjacent adsorption sites. The displacement of 1.7 Åonly induces a blurred image as observed in Fig. 7.

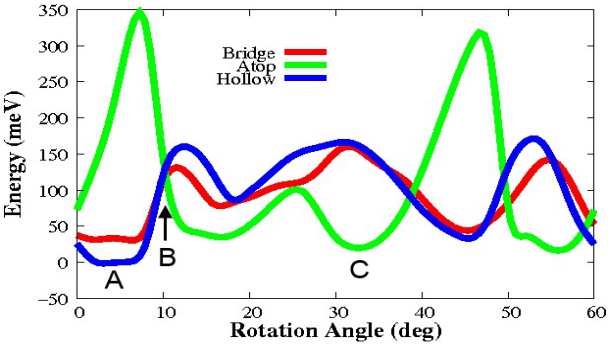

Fig. 15 Calculated rotation energy of a Ad_6HBC molecule above atop (green), hollow (blue), and bridge (red) sites of the Ag(111) surface. The curves show the adsorption energy during the rotation taking into account the relaxation of the molecule at each step.

The last point to be discussed concerns the ability to manipulate single Ad_6HBC molecules or clusters of molecules. In these manipulations, the presence of the adamantyl groups appears of fundamental importance. On the one hand, these diamondoid cages limit the interactions between the central π system and the metallic surface which favours lateral displacement. On the other hand, their quasi-spherical geometry increases the mobility on the substrate and each AD group acts as a wheel rolling on the flat Ag surface.

On previous investigations concerning Ad_6HPB molecules, this property was not observed essentially because the hexa-phenyl-benzene part does not present a flat geometry but a propeller shape[35]. As Ad_6HBC molecules feature a flat central structure (even if slightly bended), they can be more easily manipulated by the tip using the pushing mode. During these manipulations, periodic variations of the tunneling current are rarely observed. However, it is generally reported that the manipulation of single atoms or small molecules along close packed directions induces tip height modulations in accordance with atomic surface periodicities[28–33]. On the contrary, the complex and large structure of Ad_6HBC implies sophisticated displacement mechanisms which significantly differ from single atom manipulations[34]. Moreover, the manipulation signatures are difficult to interpret according to the initial position of the tip above or in front of the molecule. When regular variations of the tunneling current are observed in our experiments, their period is in the 1 nm to 1.5 nm range which is large as

compared to the Ag(111) surface parameter (0.28 nm). For example, a spatial period of 1.24 nm can be calculated from the I_t modulations observed in Fig.10c. The same values are observed for dimers or trimers manipulations. It is assumed that the flexibility of the peripheral adamantyl groups allows the detection of the substrate atomic corrugation during the molecule motion provided that the manipulation direction induced by the tip is carefully chosen. This flexibility implies the possible rotation around the C-C bond between the AD and HBC parts. This will generate periods above 1 nm since the mean diameter of an AD group is around 0.43 nm. A complete interpretation of this phenomenon implies sophisticated molecular mechanics/dynamics calculation out the scope of the paper.

Due to the peculiar structure of Ad_6HBC and particularly the flexible peripheral moieties, a specific mechanical interaction between the molecules can take place during manipulation. It is then possible to create clusters on the surface which present a high stability and result from the solid anchoring between single molecules. Thereafter, these small assemblies can be manipulated or rotated without any problem. The flexibility of the AD peripheral groups insure the mechanical cohesion of the structure without any fragmentation. The process is reversible since the STM tip may be used to remove one molecule from the cluster by increasing the tip molecule interaction during a scan. This always results in the removal of an entire molecule which can be again manipulated. In the future, this kind of manipulation can be used to build assemblies with controlled geometries or to connect single molecules to nanometric metallic wires.

5 Conclusion

Hexa-Adamantyl-Hexa-Benzocoronene molecules deposited on Ag(111) have been studied. These molecules present interesting self-assemblies properties due to their peripheral adamantyl groups and form hexagonal structures driven by van der Waals bonding. At the single molecule scale, the experimental images reveal contrast variations according to the bias voltage, showing a increased signal originating either from the adamantyl groups or the central plateau. These results have been interpreted with a great accuracy using calculated STM images. Investigations concerning rotational energy show that a single molecule can rotate under the tip which is consistent with the experimental observations. The molecules can be also manipulated on the surface and are able to form stable dimers or trimers. These clusters are formed by mechanical interactions favoured by the flexible molecular structure.

6 References

References

1 F. Rosei, M. Schunack, Y. Naitoh, P. Jiang, A Gourdon, E. Laegsgaard, I. Stensgaard, C. Joachim, F. Besenbacher, Properties of large organic molecules on metal surfaces, *Prog. Surf. Sci.* **71** (2003) 95-146.

2 E. Clar, Aromatishe Kohlenwasserstoffe-Polycyclishe Systeme, Springer,Berlin, Göttingen, Heidelberg, 1952.

3 M. Möller, C. Kübel, K. Müllen, Giant Polycyclic Aromatic Hydrocarbons, *Chem. Eur. J.* **4** (1998) 2099-2109.

4 M. Treir, P. Ruffieux, R. Schillinger, T. Greber, K. Müllen, R. Fasel, Living at the edge: a nanographene molecule adsrobed across gold step edges, *Surf. Sci.* **602** (2008) L84-L88.

5 T. Schmitz-Hubsch, F. Sellam, R. Staub, M. Torker, T. Fritz, Ch. Kubel, K. Müllen, K. Leo, Direct observation of organic-organic heteroepitaxy: perylene-tetracarboxylic-dianhydride on hexa-peri-benzocoronene on highly pyrolitic graphite, *Surf. Sci.* **445** (2000) 358-367.

6 J. Martinez-Blanco, M. Klingsporn, K. Horn, Selective adsorption of coronene on Si(111)7×7, *Surf. Sci.* **604** (2010) 523-528.

7 L. Gross, F. Moresco, P. Ruffieux, A. Gourdon, C. Joachim, K.H. Rieder, Tailoring molecular self-organization by chemical synthesis: Hexaphenylbenzene, hexa-peri-hexabenzocoronene, and derivatives on Cu(111), *Phys. Rev. B* **71** (2005) 165428-165435.

8 M. Toerker, T. Fritz, H. Proehl, R. Gutierrez, F. Grossmann, R. Schmidt, Electronic transport through occupied and unoccupied states of an organic molecule on Au: experiment and theory, *Phys. Rev. B* **65** (2002) 245422-245430.

9 M. Lackinger, S. Griessl, W.M. Heckl, M. Hietschold, Coronene on Ag(111) investigated by LEED and STM in UHV, *J. Phys. Chem. B* **106** (2002) 4482-4485.

10 F. Jäckel, Z. Wang, M.D. Watson, K. Müllen, J.P. Rabe, Nanoscale array of inversely biased molecular rectifiers, *Chem. Phys. Lett.* **387** (2004) 372-376.

11 M.D. Watson, K. Jäckel, N. Severin, J.P. Rabe, K. Müllen, A Hexa-peri-hexabenzocoronene cyclophane: an addition to the toolbox for molecular electronics, *J. Am. Chem. Soc.* **126** (2004) 1402-1407.

12 P.T. Herwing, V. Enkelman, O. Schmelz, K. Müllen. Synthesis and Structural Characterization of Hexa-tert-butyl- hexa-peri-hexabenzocoronene, Its Radical Cation Salt and Its Tricarbonylchromium Complex.

Chem. Eur. J. **6** (2000) 1834-1839.

13 D. Sun, S.V. Rosokha, J.K. Kochi. Through-Space (Cofacial) -Delocalization among Multiple Aromatic Centers: Toroidal Conjugation in Hexaphenylbenzene-like Radical Cations. *Ang. Chem.* **44** (2005) 5133-5136.

14 S. Choua, A. Jouaiti, M. Geoffroy. An EPR/ENDOR study of the reduction products of symmetrical isomers of dipyridylacetylene. *Phys. Chem. Chem. Phys.* **15** (1999) 1557-1560.

15 J. Bormann, M.R. Gold, W. Schatton. US patent 5061703 (1990).

16 H. Suzuki. Direct Iodination of Polyalkylbenzenes: iododurene. *Org. Synth.* **51** (1971) 94.

17 N. L. Allinger, K. S. Chen, J. H. Lii, An improved force field (MM4) for saturated hydrocarbons. *J. Comput. Chem.* **17** (1996) 642-668.

18 N. L. Allinger, Understanding moleular structure from molecular mechanics. *J. Comput. Aided Mol. Des.* **25** (2011) 295-316.

19 T. Zambelli, S. Goudeau, J. Lagoute, A. Gourdon, X. Bouju, S. Gauthier, Molecular self-assembly of jointed molecules on a metallic substrate: from single molecule to monolayer, *ChemPhysChem* **7** (2006), 1917-1920.

20 M. Yu, N. Kalashnyk, W. Xu, R. Barattin, Y. Benjalal, E. Lægsgaard, I. Stensgaard, M. Hliwa, X. Bouju, A. Gourdon, C. Joachim, F. Besenbacher, T. R. Linderoth, Supramolecular Architectures on Surfaces Formed through Hydrogen Bonding Optimized in Three Dimensions, *ACS Nano* **4** (2010) 4097-4109.

21 M. Yu, W. Xu, N. Kalashnyk, Y. Benjalal, S. Nagarajan, F. Masini, E. Lægsgaard, M. Hliwa, X. Bouju, A. Gourdon, C. Joachim, F. Besenbacher, T. R. Linderoth, From zero to two dimensions: supramolecular nanostructures formed from perylene-3,4,9,10-tetracarboxylic diimide (PTCDI) and Ni on the Au(111) surface through the interplay between hydrogen-bonding and electrostatic metal-organic interactions, *Nano Res.* **5** (2012) 903-916.

22 P. Sautet, C. Joachim. Calculation of the benzene on rhodium STM images. *Chem. Phys. Lett.* **185** (1991) 23-30.

23 M. Yu, W. Xu, Y. Benjalal, R. Barattin, E. Lægsgaard, I. Stensgaard, M. Hliwa, X. Bouju, A. Gourdon, C. Joachim, T. R. Linderoth, F. Besenbacher. STM manipulation of molecular moulds on metal surfaces. *Nano Res.* **2** (2009) 254-259.

24 B. Calmettes, S. Nagarajan, A. Gourdon, Y. Benjalal, X. Bouju, M. Abel, L. Porte, R. Coratger. Properties of Penta-*tert*-butylcorannulene Molecules Inserted in Phthalocyanine Networks Studied by Low-Temperature Scanning Tunneling Microscopy. *J. Phys. Chem. C* **113** (2009) 21169-21176.

25 C. Manzano, W. H. Soe, M. Hliwa, M. Grisolia, H. S. Wong, C. Joachim. Manipulation of a single molecule ground state by means of gold atom contacts. *Chem. Phys. Lett.* **587** (2013) 35-39.

26 H. Cercelier, Y. Fagot-Revurat, B. Kierren, D. Malterre, F. Reinert, Shockley state in epitaxial Ag films on Au(111), *Surf. Sci.* **566** (2004) 520-525.

27 F. Moresco, G. Meyer, K.-H. Rieder, H. Tang, A. Gourdon, C. Joachim. Low temperature manipulation of big molecules in constant height mode. *Appl. Phys. Lett.* **78** (2001) 306-308.

28 X. Bouju, C. Joachim, C. Girard, H. Tang. Mechanics of $(Xe)_N$ atomic chains under STM manipulation. *Phys. Rev. B* **63** (2001) 085415.

29 S.-W. Hla, K.-F. Braun, K.-H. Rieder. Single-atom manipulation mechanisms during a quantum corral construction. *Phys. Rev. B* **67** (2003) 201402.

30 M. Alemany, L. Gross, F. Moresco, K.-H. Rieder, C. Wang, X. Bouju, A. Gourdon, C. Joachim. Recording the intramolecular deformation of a 4-legs molecule during its STM manipulation on a Cu (211) surface. *Chem. Phys. Lett.* **402** (2005) 180-185.

31 L. Bartels, G. Meyer, K.-H. Rieder. Basic steps of lateral manipulation of single atoms and diatomic clusters with a scanning tunneling microscope tip. *Phys. Rev. Lett.* **79** (1997) 697-700.

32 X. Bouju, C. Joachim, C. Girard. Single-atom motion during a lateral STM manipulation. *Phys. Rev. B* **59** (1999) 7845-7848.

33 S.W. Hla, Scanning tunneling microscopy single atom/molecule manipulation and its application to nanoscience and technology), *J. Vac. Sci. technol. B* **23** (2005) 1351-1360.

34 L. Grill, K.-H. Rieder, F. Moresco, G. Rapenne, S. Stojkovic, X. Bouju, C. Joachim. Rolling a single molecular wheel at the atomic scale. *Nat. Nanotech.* **2** (2007) 95-98.

35 R. Coratger, B. Calmettes, Y. Benjalal, X. Bouju, C. Coudret, Structural and electronic properties of hexa-adamantyl-hexa-phenylbenzene molecules studied by low temperature scanning tunneling microscopy, *Surf. Sci.* **606** (2012) 444-449.

36 J.C. Garcia, J.F. Justo, W.V.M. Machado, L.V.C. Assali, Functionalized adamantane: Building blocks for nanostructure self-assembly, *Phys. Rev. B* **80** (2009) 125421-125426.